

The detection of possible γ -ray quasi-periodic modulation with ~ 600 days from the blazar S2 0109+22

HAOYANG ZHANG ¹, FAN WU ¹ AND BENZHONG DAI ¹

¹*Department of Astronomy, Key Laboratory of Astroparticle Physics of Yunnan Province, Yunnan University, Kunming 650091, China*

ABSTRACT

In this work, we analyzed the long-term γ -ray data by a Fermi Large Area Telescope (Fermi-LAT) of blazar S2 0109+22, ranging from 2008 to 2023. The quasi-periodic oscillations (QPOs) of blazars aided in investigating the physical properties of internal supermassive black holes, the nature of variability, and the underlying radiation mechanism. We employed four different methods—Weighted Wavelet Z-transform, Lomb-Scargle periodogram, REDFIT and phase folded light curve analysis, for searching QPO signals. Our analysis identified a possible QPO behavior with a periodicity of ~ 600 days in November 2013 to January 2023 at a significance level of $\sim 3.5\sigma$. This QPO signal sustained ~ 9 years, corresponding to 5.6 cycles, which was in good agreement with the previously observed of periodicity ~ 657 days in radio. We explained this phenomenon based on the accretion model and the lighthouse effect, in a binary black hole system.

Keywords: galaxies: active — BL Lacertae objects: individual (S2 0109+22) — gamma rays: galaxies — galaxies: jets

1. INTRODUCTION

Active galactic nuclei (AGN) emits extreme non-thermal and thermal radiation across all-wavelengths, from radio to high energy γ -rays. AGNs are generally considered as accretion systems with a supermassive black hole (SMBH) at their centre, providing the necessary power (Padovani et al. 2017). AGNs can be classified into jetted and non-jetted (Padovani 2017). When the jet is oriented close to our line of sight, it form the subclass called the blazars (Urry & Padovani 1995). Blazars are classified into BL Lacertae objects (BL Lacs) and flat spectrum radio quasars (FSRQs). Generally, blazars always have a variability in all-wavelengths with different timescales (Wagner & Witzel 1995; Dai et al. 2001, 2009, 2015). According to the variability timescale, the variability is categorized into intraday variability with the timescales of a single day, the short-term variability with timescales of a few days to months, and the long-term variability with timescales of years (Fan et al. 2011, 2021; Cai et al. 2022).

With the increase of observational data, a special variability phenomenon of quasi-periodic oscillations

(QPOs) has been discovered in AGNs across all energy spectrum. For non-jetted AGNs, which comprise the majority of existing AGNs, quasi-periodic behavior has been observed in both optical and X-ray emissions. This quasi-periodic behavior has been associated with the accretion disk emission and usually occurs over the time scales of hours to months, such as ~ 44 days in KIC 9650712 (Smith et al. 2018), ~ 1 hour in RE J1034+396 (Gierliński et al. 2008), ~ 2 hours in Mrk 766 (Zhang et al. 2017a). Harmonic oscillations with the ratios of 1:2 and 1:3 have been detected in 1H 0707-495 and Mrk142, respectively (Zhang et al. 2018; Zhang 2021). These QPOs can often be interpreted as models of orbital resonances (Abramowicz et al. 2003; Horák 2008; Zhou et al. 2015). In this scenario, the states of particles along different directions on the accretion disk (i.e., orbital, vertical, and radial epicyclic) are coupled to create resonance. A doubt about the applicability of this model to AGNs has been raised by Smith et al. (2021). There are certain alternative models that have been proposed, such as the seismic models (Perez et al. 1997; Rezzolla et al. 2003), the accretion disk hot spot models (Schnittman & Bertschinger 2004), and a transient chaos accretion model called the “Dripping Handrail” (Scargle et al. 1993; Young & Scargle 1996). Therefore, studying the QPO behavior in non-jetted AGNs is crucial for understanding the physical structure of SMBH

accretion systems. Further observational data is needed to support the possible physical explanations.

The jetted AGNs exhibit strong non-thermal radiation from relativistic jets. In the radio band of 15 GHz, the periodic signals from a few hundred days to several years have been reported, i.e., ~ 150 days in J1359+4011, ~ 270 days for blazar PKS 0219-164, 4.69 years in PKS J2134-0153, and 965 days for AO 0235+164 (14.5 GHz) (King et al. 2013; Bhatta 2017; Ren et al. 2021; Tripathi et al. 2021). In the optical, OJ 287 has been identified as the most likely candidate for a binary black hole system with a 12 years period (Sillanpaa et al. 1985, 1988; Valtonen et al. 2006, 2008), and certain shorter periodic signals of ~ 400 and ~ 800 days have been reported in OJ 287 (Bhatta et al. 2016). In addition, the periodic signals of ~ 317 days, ~ 283 days and 6.4 years for PKS 2155-304, 1823+568 and SDSS J0752, have been reported (Zhang et al. 2014; Li et al. 2022; Zhang 2022). Thanks to the Fermi Large Area Telescope (Fermi-LAT) for the long-term monitoring of blazars in gamma-ray energy, the first gamma-ray QPO signal of 2.18 years have been found in blazar PG 1553+113 (Ackermann et al. 2015). Recently, about 30 blazars showing QPO signals have been discovered by employing multiple techniques. The timescale falls in the range of months-like oscillations of 34.5 days to several years (Ackermann et al. 2015; Sandrinelli et al. 2017; Zhang et al. 2017b,c,d; Zhou et al. 2018; Kushwaha et al. 2020; Peñil et al. 2020; Wang et al. 2022; Ren et al. 2023). The monthly timescale modulation is considered to be the helical structure of the jet, and the periodic signals are generated while the viewing angle of the emission region changes (Zhou et al. 2018). The presence of a binary black hole system is the leading theory for a galaxy with a long-term periodicity with in the order of years QPO behavior (Lehto & Valtonen 1996; Sandrinelli et al. 2014; Ren et al. 2021). Thus the Kepler-orbit causes the change in the angle between the jet and observer directions, and the Doppler factor changes cause the periodic phenomenon (Sobacchi et al. 2017; O’Neill et al. 2022). Furthermore, the Lense-Thirring precession of the accretion disk can also produce the quasi-periodic phenomena of the annual time scale (Bhatta & Dhital 2020). For blazars, the precession of the accretion disk can also affect the jet flow, which leads to the periodic flux variations (Liska et al. 2018). Black hole and accretion disk are the energy sources of jet (Blandford & Znajek 1977; Blandford & Payne 1982). Accretion disks may create or destroy QPOs from the jets (Liu et al. 2006). The results of these models are in good agreement with the observations, though further evidence is required in support for these models.

Most of the traditional tools for searching the periodic signals are based on Fourier technique, such as Discrete Fourier Transform (Ferraz-Mello 1981; Foster 1995), Lomb–Scargle periodogram (Lomb 1976; Scargle 1982), Weighted Wavelet Z-transform (Foster 1996). Fourier techniques are sensitive to sinusoidal variations, but the QPO behaviors of X-ray binaries are considered non-sinusoidal and harmonic (Ingram & van der Klis 2015). Therefore, the results obtained using these methods may be inaccurate and unreliable. Recently, methods based on Gaussian processes have been proposed (Kelly et al. 2014; Foreman-Mackey et al. 2017). Furthermore, because the telescope observations span a short time, the methods and criteria for confirming a high-significance QPO remain controversial, thus making the QPO analysis in AGNs complicated (Covino et al. 2019; Yang et al. 2021; Zhang et al. 2023).

S2 0109+22 (GC 0109+224, TXS 0109+224, RXJ0112+2244) is a compact radio-loud AGN at coordinates (J2000) RA=01h12m05.8s and DEC=+22d44m39s. It was first identified as a compact radio object by Davis (1971) and Pauliny-Toth et al. (1972) using National Radio Astronomy Observatory (NRAO) 43-m dish of Green Bank in the 5 GHz. The work Wills & Wills (1976) has analyzed the spectra of S2 0109+22 and did not find the absorption or emission lines, and it shows the characteristics of a BL Lac object. Owen & Mufson (1977) have measured a strong millimeter-wave emission in the 90 GHz and defined it as a BL Lac object. The work Pica (1977) suggest that S2 0109+22 is an intermediate in the type between the large-amplitude variables (OJ 287) and the smaller-amplitude objects (ON 235, OY 091). The latest redshift estimate is $z \sim 0.36$ (MAGIC Collaboration et al. 2018).

The source S2 0109+22 has reportedly shown the possible periodic flux variation in radio band Ciprini et al. (2004). By employing University of Michigan Radio Astronomy Observatory (UMRAO) and Metsahovi Radio Observatory data (since 1976 to 2002), they found QPO signals of 3.74 and 4.16 years in 37 and 22 GHz, respectively, 3.43 and 1.8 years in 14.5 GHz, all of results with the significance of $>99\%$. Except these, there are no other QPO reported in a different energy band. The search for the QPO behavior, helps us to understand the characteristics and mechanisms of the variability of this blazar. Further, the Fermi-LAT could support the long-term observation in the search for the QPO signals.

In this paper, we searched for the S2 0109+22 period variation by employing the γ -ray data of Fermi LAT. In Section 2, we have introduced the observation and data reduction in the γ -ray energy bands. In Section 3, we

briefly introduce the periodic search methods and give the analysis results. In Section 4, we have discussed the application of the binary black hole model of accretion and lighthouse effect. In Section 5, we have given the conclusion of our work.

2. OBSERVATIONS AND DATA REDUCTION

Fermi-LAT can survey the whole sky region with in the energy range of 20 MeV to 300GeV for every three hours (Atwood et al. 2009). It has made long-term observations of S2 0109+22 (4FGL J0112.1+2245) from 2008-2023 (Abdollahi et al. 2020). We have selected the events file in 2008 August 4 to 2023 January 16 (54682-59974 MJD) from the Fermi Pass 8 database.¹ The standard criteria for data reduction is the point-source analysis and the analyzing tool is the official software Fermitools 2.0.8.² Concerning the details of the process, the region of interest (ROI), filter expression and maximum zenith angle value have been used as 15° , (DATA_QUAL>0) & (LAT_CONFIG=1), 90° , respectively. In the likelihood analysis, we select `gll_iem_v07.fits` and `iso_P8R3_SOURCE_V3_v1.txt` as the Galactic diffuse emission model file and the extragalactic isotropic diffuse emission model file, respectively. The instrumental response function is `P8R3_SOURCE_V3`. Furthermore, the data of S2 0109+22 in 0.1-300 GeV have been selected for the binned maximum-likelihood analysis. We have obtained an average photon flux $(8.37 \pm 1.54) \times 10^{-8}$ photons $cm^{-2} s^{-1}$ and the test statistic (TS) value is ~ 28872.4 . The corresponding best-fit spectral parameters are $\alpha = 2.01 \pm 0.01$, $\beta = 0.05 \pm 0.01$ and $E_b = 0.769$ GeV with LogParabola model using Fermitools software.

Following the determination of the model file with the binned likelihood analysis, we have conducted the unbinned likelihood analysis with 7-day binned. The choice of the 7-day binned has provided the shortest time intervals that can have enough data points to characterize the flux over time, with the maximum likelihood Test Statistic (TS) values exceeding 9 ($\sim 3\sigma$). The light curve of S2 0109+22 is displayed in top panel of Figure 1, where only the flux with the TS>9 is plotted. To verify the reliability of periodicity, we have adopted the same operation process to extract the 10-day binning and 30-day binning light curves for the analysis.

3. DATA ANALYSIS AND RESULTS

3.1. Methods

To study the variability properties of S2 0109+22 in γ -ray energy, four different methods have been applied to search for the periodic signals in the gamma-ray light curve. Weighted Wavelet Z-transform (WWZ, Foster (1996)) fit the sinusoidal waves that are localized in both the frequency and time domains. It has the advantage of showing the evolution of the peak frequency over time. This method gives the 2D time-frequency power map and time average power spectrum. The Lomb-Scargle periodogram (LSP, Lomb (1976); Scargle (1982)) is a technique similar to the Fourier transform. It can calculate the power spectrum of non-equally spaced sampling time series by assuming a sine function for the periodic component. We employed this method for verifying the periodic behavior found by WWZ. The REDFIT software³ has been developed by Schulz & Mudelsee (2002). In this method, the power spectral density (PSD) of time series has been calculated based on the LSP. The red noise level of the PSD has been estimated by fitting a first-order autoregressive process. The advantage of this method is that it can accurately estimate the significance of the broad peak structure in PSD under the red noise background. A light curve folded at a suspicious period should have an approximate periodic shape by using the phase folded light curve. For the Fermi-LAT data, we have used the phase-resolved binned likelihood analysis with the obtained period.

We have used the *baluev* method given by Baluev (2008) to describe the False Alarm Level (FAL) of the peak given by LSP, and to estimate the FAL of the peak in PSD (see the red dashed line in Figure 2). To eliminate the noise from the false periodic signal, we have employed the light curve simulation software⁴ developed by Emmanoulopoulos et al. (2013) to estimate the significance of the result. This technique is based on the assumption that the PSD of AGN is a red noise spectrum (Timmer & Koenig 1995), henceforth giving the simulated light curve by fitting the PSD and probability density function (PDF) of the light curves. We have simulated 10^5 light curves for the LSP method and WWZ method to calculate the significance level of these results.

3.2. Results

WWZ can reveal the dynamic fluctuation of the power spectrum over time. The results of WWZ analysis on the data are shown in Figure 1. We have shown the 7 days bin^{-1} complete time span light curve (54682-59974 MJD) and the corresponding WWZ power dia-

¹ https://fermi.gsfc.nasa.gov/ssc/data/analysis/documentation/Pass8_usage.html

² <https://github.com/fermi-lat/Fermitools-conda/>

³ <https://www.manfredmudelsee.com/soft/redfit/index.htm>

⁴ <https://github.com/samconnolly/DELightcurveSimulation>

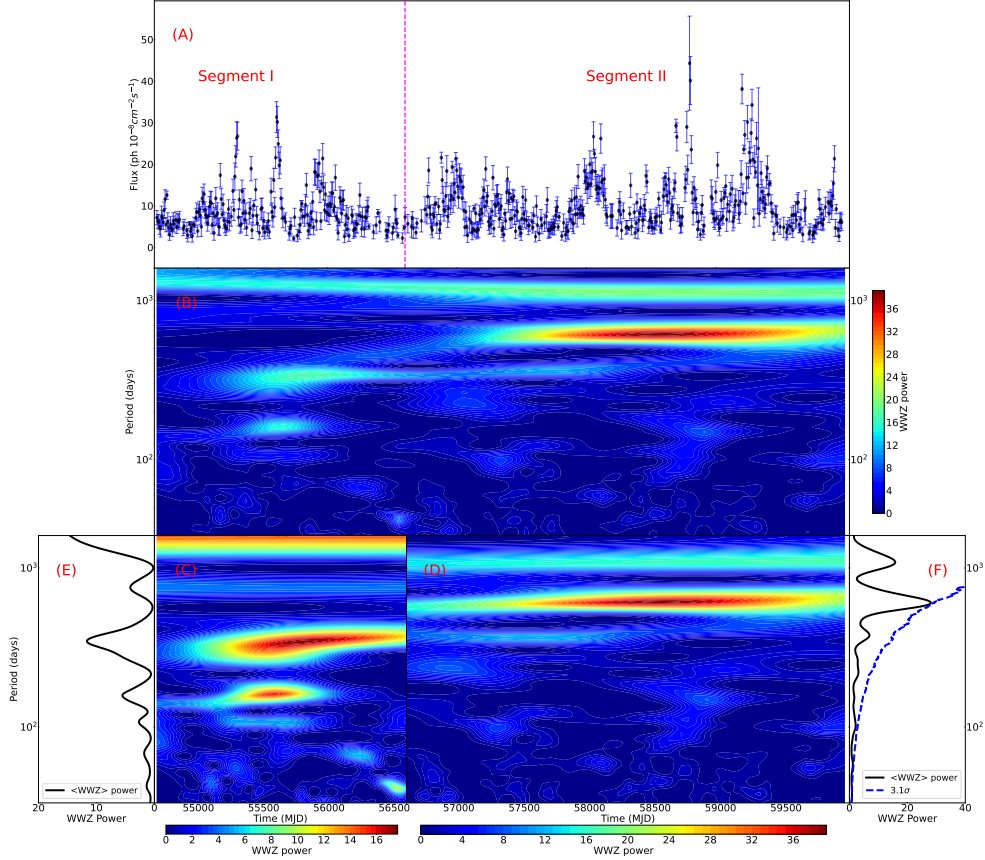


Figure 1. Panel (A) is the Fermi-LAT 0.1-300 GeV γ -ray light curve with 7-day binned from MJD 54682 to 59974 and the error bar represent $TS > 9$ data. The pink dashed line shows the time after which the periodic behavior occurs (Segment II, 56600-59974 MJD). Panel (B) indicates the WWZ 2D analysis results of the complete time span light curve. The results of Segments I and II analysis using WWZ are shown in panels (C) and (D). The corresponding average WWZ power with Segments I and II is expressed by panels (E) and (F), respectively. The black line represents the average WWZ power and the blue dashed line represents the 3.1σ significance level.

gram, in the panels (A) and (B) of Figure 1. The power increase can be seen in the Segment II (56600-59974 MJD), for a time scale of ~ 600 days. To analyse the periodic behavior accurately, we have analysed Segment I (54682-56600 MJD) and Segment II with WWZ. Panels (D) and (F) show the WWZ 2D map and the average power of Segment II, respectively. We have obtained 604 ± 78 days of periodic signals with 3.1σ significance level about average WWZ power. The uncertainty range of the period was the full width at half maxima (FWHM) of the peak fitted by a Gaussian function. We also used the same operations for Segment I (see in panel (C) and panel (E)). Although it shows a short periodic behavior, the significance was less than 2σ . We did not consider this transient periodic behavior in the subsequent discussions.

We have found a period of 596 ± 62 days (see in Figure 2) from the LSP analysis results of MJD 56600 to 59974

(Segment II). The peak exceeds 99.99% FAL and achieve 3.5σ significance.

The result of analysis from the Segment II using REDFIT program is shown in Figure 3. The peak was well above 99% significance level at 588 ± 80 days. Although the period was slightly short than those of the previous two methods, they were within the allowable error range of the value.

To confirm the reliability of our results, a phase folded technique has been employed for validation. Figure 4 shows, the significant periodic shape when we fold it over a period of 600 days from 56685 to 59685 MJD.

Four methods have been found to have a significant quasi-periodic behavior with ~ 600 days at 56600-59974 MJD, with the LSP giving a significance level of about 3.5σ and well above 99.99% FAL. We list the results of search for the periodic signals using four methods, in Table 1. We have also analyzed the data of 10 days bin^{-1} and 30 days bin^{-1} of S2 0109+22. The quasi-

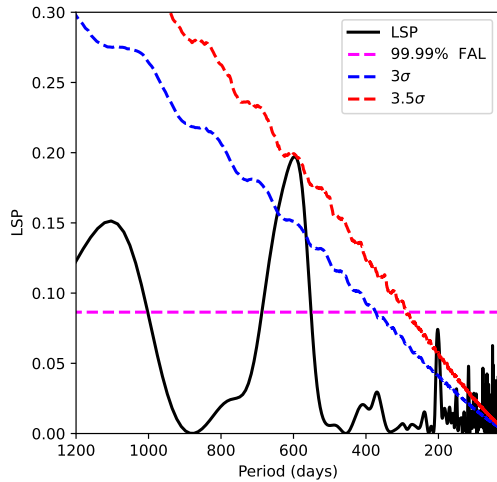


Figure 2. Possible period obtained from LSP in Segment II. The black line is the LSP power, in which a broad peak with peak value of 596 ± 62 days. The dashed red, blue, and pink lines correspond to the 99.99% FAL, 3σ and 3.5σ significance levels, respectively.

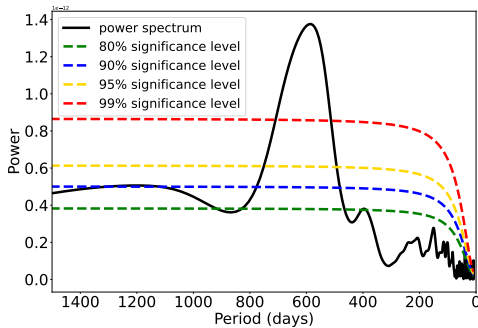


Figure 3. Results from analysis of the REDFIT program. The black line is the PSD calculated by REDFIT, the peak value is 588 ± 80 days. The dashed lines with green, blue, yellow and red colors indicate the significance level by estimating the red noise background.

periodic behavior of ~ 600 days was found to be evident after different time cadence.

4. DISCUSSION

The long-term γ -ray data have been analyzed using four different techniques to look for periodicity. These methods delivered consistent results. Previously, Ciprini et al. (2004) reported that this source had a radio quasi-periodic modulation of ~ 657 days with a $>99\%$ confidence level. In our work, the periodicity of the two energy bands is consistent while considering the error

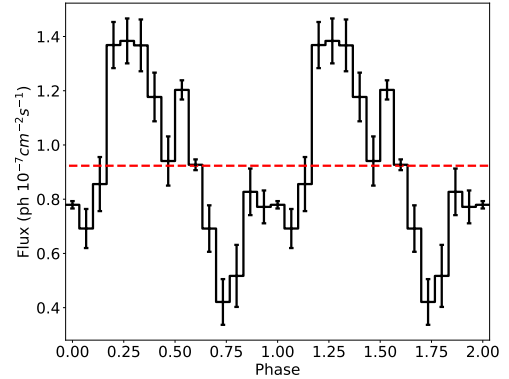


Figure 4. Phase folded light curve with period of 600 days existed in Segment II, from 56685 to 59685 MJD. Two clarified cycles are shown. The dashed red line is the mean flux.

range, which strongly supports our finding. Figures 1 (F) and 2 show that another peak has been detected at a location of approximately 1100 days with a FAL above 99.99%, though the simulated light curves clearly gave a result that was below the 3σ significance level. We generally considered signals that exceeded both of the significance estimation methods are reliable. This may be because the analysis methods were based on the Fourier transform and decomposed the original signal into a sum of frequency components, including harmonic frequencies (Wang et al. 2022). Therefore, in the following discussion, we did not consider it to be a real signal, but rather a frequency doubling of the detected QPO. Consequently, we confirmed that there was an obvious periodic behavior for BL Lac S2 0109+22 in γ -ray with 3.5σ significance level of ~ 600 days (1.64 years).

In Segment I, we found no evidence of a periodic activity. The γ -ray light curve PDF of S2 0109+22 exhibited a significant lognormal distribution shape (see in Figure 5). Lognormal distribution will typically be visible in the PDF of X-ray binaries with the accretion disk emission dominating them (Gandhi 2009). The accretion disk and the jet radiation may have significant connections (Ricci et al. 2022; Xiao et al. 2022; Zhang et al. 2022). The accretion disk's instability caused turbulence disturbance to emerge at random in various radii. Such an effect will spread from the outside to the inside of the disk. Once it hits the innermost region, it may impact the soft photon field and electron injection into the jet, which in turn effect the emission of the jet (Lyubarskii 1997; Arévalo & Uttley 2006). The extremely high bulk Lorentz factor of the jet had the potential to enhance the effect of the accretion disk and subsequently may cause significant variations in γ -ray radiation. This scenario

Table 1. Results of the QPO analysis with 4 methods

Method	UMRAO 14.5 GHz (1980-2002)	Fermi-LAT γ -ray (2014-2022)	Significance level
WWZ		604 ± 78 days	3.1σ
LSP	~ 657 days	596 ± 62 days	3.5σ
REDFIT		588 ± 80 days	$>99\%$
phase folded light curve		~ 600 days	

NOTE—The result of UMRAO 14.5 GHz is taken from [Ciprini et al. \(2004\)](#) and the significance value is $>99\%$.

could be a factor in the periodic signals disappearing from Segment I.

To investigate scenario, we have applied the Leptonic Model (LM) to explore possible evidence for this ([Maraschi et al. 1992](#); [Sikora et al. 1994](#); [Massaro et al. 2006](#); [Tramacere et al. 2011](#); [Böttcher et al. 2013](#)). Considering that the accretion disk provides the external seed photons, we use the External Compton (EC) model to fit the γ -ray Spectral Energy Distribution (SED) of this source ([Blandford & Levinson 1995](#); [Bednarek 1998](#)). A powerful SED fitting software—JetSet⁵ ([Tramacere 2020](#)), has been employed to fit the SED of Segment I, Segment II and Total, respectively. During the fitting process, we had to freeze certain parameters to the typical values found in blazars owing to the lack of multiwavelength data. We found that the LogParabola electron spectral was the most suitable one. In Figure 6, there was an obvious spectral hardening in Segment II compared to Segment I. Under the broadly similar radiation region size ($\sim 1.4 \times 10^{15}$ cm), the electron density increases from Segment I to Segment II (from 1.99 ± 0.46 to 5.64 ± 0.14 , with units of 10^4 cm^{-3} as shown in Table 2). These parameters exhibit a similar order of magnitude as the constraints on physical parameters of high-energy radiation in blazars by [Tavecchio et al. \(1998\)](#). The accretion disk could inject electrons into the bottom of the jet ([Romero & Gutiérrez 2020](#)). Consequently, the electrons in the radiant region that were close to the black hole may be affected by the accretion disk. If the changes in the electrons proceeded from perturbations in the accretion disk, then the seed photons were affected. The periodic phenomenon in Segment II gradually gained strength over time, which may ensue from the dissipating perturbations (see in Figure 1 (A)). We performed a simple quantitative analysis of this scenario, because further study was beyond the scope of this work and requires multiwavelength SED.

⁵ <https://github.com/andreatramacere/jetset>

The long-scale quasi-periodic behavior of blazars is often interpreted as the supermassive binary black hole (BBH) systems ([Sillanpaa et al. 1988](#); [Lehto & Valtonen 1996](#); [Fan et al. 2007](#); [Sandrinelli et al. 2014](#)). This scenario consists of two parts, viz., the accretion and jet lighthouse models. In the accretion model, when the secondary black hole is close to the primary black hole owing to orbital motion, the accretion rate increases significantly, hence the flux will rise periodically ([Wang et al. 2022](#)). The jet lighthouse model considers that the periodic change of the observation angle brings about the change of the Doppler factor, thus generating the periodicity of the flux ([Villata et al. 1998](#); [Qian et al. 2007](#)). These models provide a geometric explanation for periodic behavior without relying on specific physical parameters.

First, we needed to calculate the periodic expansion due to the redshift effect which was the formula $T_{sou} = T_{obs}/(1+z)$. Then we applied the first model described above to estimate the distance between the two black holes, and considered the motion of BBH in the case of Kepler orbits, given as:

$$P_{orbital}^2 = \frac{4\pi^2 d^3}{G(M+m)} \quad (1)$$

where d represents the distance between two black holes, and M and m is the primary black hole mass and secondary black hole mass, respectively. G represents the universal gravitational constant. By substituting the redshift $z = 0.36$ of this source ([MAGIC Collaboration et al. 2018](#)). Furthermore, owing to the periodic flux from the orbital effects, we set $P_{orbital} = T_{sou} = 1.21$ years. The average black hole mass of blazar is $\bar{M} = 10^{8.6} M_{\odot}$ given by [Ren et al. \(2021\)](#). Furthermore, by assuming $m/M \sim 0.001$ by [Wang et al. \(2022\)](#), we calculated the distance between two black holes as $d = 1.25 \times 10^{16}$ cm.

In the lighthouse model, the periodicity originated from the orbital effect of the BBH, which affected the emission toward to the observer. Thus, the orbital period is equal to the QPO existing in the light curve. Gen-

erally, the light curve showed a double flare peak structure (Qian et al. 2007; Fan et al. 2021; Wang et al. 2022). This suggested a possible binary black hole jet structure. Hence, we assume that this is a binary black hole system with a dual jet. Furthermore, we set component-1 for the primary black hole and component-2 for the secondary black hole. The observation angle of two jets changing with time can be Qian et al. (2007) expressed as:

$$\cos \theta_1(t) = \sin \psi_1 \cos(\omega t + \phi_1) \sin i + \cos \psi_1 \cos i \quad (2)$$

$$\cos \theta_2(t) = \sin \psi_2 \cos(\omega t + \phi_2) \sin i + \cos \psi_2 \cos i \quad (3)$$

where ϕ_1 and ϕ_2 are the azimuths angles between the observer and jet axis of two components on the orbital plane. The two angles are expressed as the initial phase of the two periodic jet radiation. The difference of those is the interval between the two flares. According to the works (Qian et al. 2007; Fan et al. 2021; Wang et al. 2022), we set $t = 0$, the azimuths angle between the observer and component-1 is $\phi_1 = 80^\circ$ and $\phi_2 = 240^\circ$ for component-2, according to the shape of the flux variability. The angles between jet axis and orbital axis for component-1 and component-2 were ψ_1 and ψ_2 , respectively. Furthermore, i was set as the sight direction with the orbital axis and the parameter ω was calculated based on $(2\pi/T_{obs})$. Therefore, we obtained the representation of the variable Doppler factors (δ_1 and δ_2):

$$\begin{aligned} \delta_1(t) &= [\Gamma_1(1 - \beta_1 \cos \theta_1(t))]^{-1} \\ \delta_2(t) &= [\Gamma_2(1 - \beta_2 \cos \theta_2(t))]^{-1} \end{aligned} \quad (4)$$

where $\Gamma = (1 - \beta^2)^{-1/2}$ is the Lorentz factor and, β is the bulk velocity of the jet in the unit of light speed. The apparent velocity (β_{app1} and β_{app2}) are (Xiao et al. 2019; Wang et al. 2022):

$$\begin{aligned} \beta_{app1}^2(t) &= -\delta_1(t)^2 - 1 + 2\delta_1(t)\Gamma_1 \\ \beta_{app2}^2(t) &= -\delta_2(t)^2 - 1 + 2\delta_2(t)\Gamma_2 \end{aligned} \quad (5)$$

The changed flux caused by the change of Doppler factors are given as:

$$f_1(t) = f_{b1}\delta_1(t)^4, \quad f_2(t) = f_{b2}\delta_2(t)^4 \quad (6)$$

where f_{b1} and f_{b2} are the normalization constant of the light curve fitting.

Following the determination the QPO timescale, the lighthouse model has been used to fit the light curve.

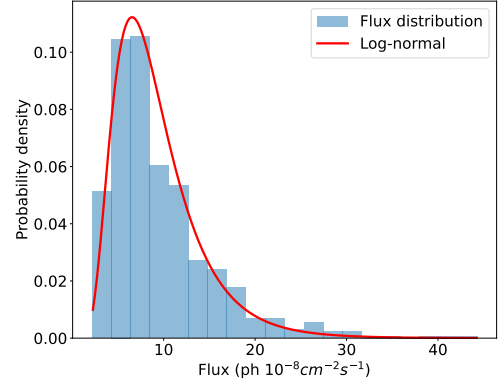


Figure 5. Histogram shown as the flux PDF of γ -ray light curve of S2 0109+22. The red line is the lognormal distribution fit with the parameters $s = 0.48$ and $scale = 8.26$ by the Python package `scipy.stats.lognorm`.

We used the `iminuit` program⁶ (Dembinski & et al. 2020) for maximum likelihood fitting of the data. The fitting parameters are shown in Table 3. The reduced χ^2 of the model is 1.67 obtained by `iminuit`. The model agreed the overall trend of the curve, and the points outside the model were proximate to the model curve without considerable deviation (see in Figure 7). As mentioned previously, the jet radiation was affected by various factors such as internal instability of accretion disk, hence it was difficult for a simple BBH jet model to fit perfectly. We also gave the law of Doppler factors ($\delta_1(t)$, $\delta_2(t)$) and apparent velocities (β_{app1} , β_{app2}) changing with time in the Figure 8. The periodic change of Doppler factor caused the formation of quasi-periodic signal and, in turn, the periodic change of apparent velocity.

The best fitting of the Doppler factor range of component-1 and component-2 were $1.67 < \delta_1 < 8.66$ and $1.10 < \delta_2 < 3.80$, respectively. Fan et al. (2013) have estimated the Doppler factors of 138 Fermi blazars, where the result for S2 0109+22 is $\delta_\gamma = 2.59$. Our model fitting parameter of Doppler factor was compatible with this result. We also obtained the apparent velocity range with $10.62 < \beta_{app1} < 23.02$ for component-1 and $8.65 < \beta_{app2} < 15.83$ for component-2. Xiao et al. (2019) have suggested that the latest range of superluminal velocity was $0.53 < \beta_{app} < 34.80$, and our result fell within this range.

Because the γ -ray flux distribution was lognormal, we speculated that the disturbance of the accretion disk to the jet may caused the periodic disappearance in the

⁶ <https://iminuit.readthedocs.io/en/stable/about.html>

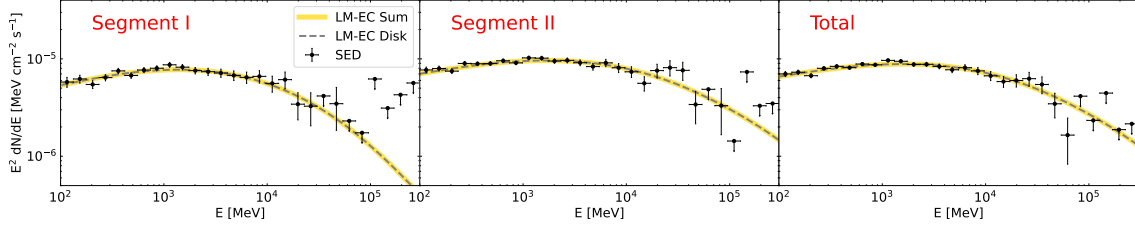


Figure 6. Segments I and II, and Total SED are represented by black error bars for the left, middle, and right panels, respectively. The gray dashed and yellow lines shown the SED fitting results of the accretion disk contribution and the sum of each component contributions in LM, respectively.

Table 2. Parameters for the LM Model.

Parameter	Segment I	Segment II	Total	Reference
Electron Density ($1/cm^3$)	$(1.99 \pm 0.46) \times 10^4$	$(5.64 \pm 0.14) \times 10^4$	$(5.27 \pm 0.74) \times 10^4$...
Radiation Region Size (cm)	$(1.51 \pm 0.20) \times 10^{15}$	$(1.30 \pm 0.21) \times 10^{15}$	$(1.52 \pm 0.13) \times 10^{15}$...
Electron Spectral Slope	2.34 ± 0.07	2.45 ± 0.04	2.46 ± 0.02	...
Electron Spectral Curvature	$(1.60 \pm 0.53) \times 10^{-1}$	$(-2.17 \pm 0.07) \times 10^{-1}$	$(-2.09 \pm 0.03) \times 10^{-1}$...
Electron Spectral cut-off Γ	$(1.90 \pm 0.56) \times 10^2$	$(8.27 \pm 1.33) \times 10^4$	$(4.51 \pm 0.40) \times 10^4$...
Radiation position* (cm)		5×10^{14}		1
Γ^*		35		2
M_{BH}^*		$10^{8.6} M_{\odot}$		3
z^*		0.36		4
L_{disk}^* (erg/s)		1×10^{45}		5
\dot{M}/\dot{M}_{edd}		0.12		5
Reduced χ^2	0.88	1.25	1.53	...

NOTE—References: (1) Tramacere et al. (2009), (2) Wang et al. (2022), (3) Ren et al. (2021), (4) MAGIC Collaboration et al. (2018), (5) Donea & Protheroe (2003). The superscript “*” indicates the frozen parameter in fit.

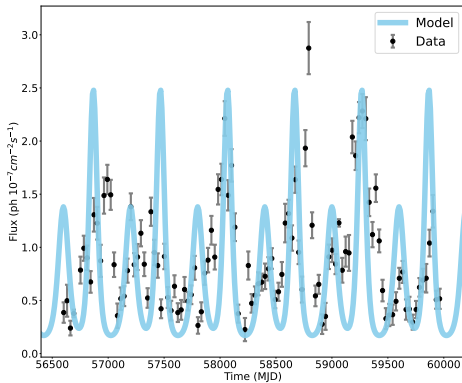


Figure 7. Fitting the lighthouse model. The light blue line indicates the results of lighthouse model fitting, and the gray error bar shows the 30 days bin^{-1} data from Fermi-LAT.

Segment I. Periodic accretion model and binary black

hole lighthouse model have been employed to explain this quasi-periodic phenomenon. The lighthouse model could not fit all the data points perfectly. Therefore, we believed that this quasi-periodic phenomenon was dominated by the variable Doppler factor caused by dual jets, whereas the periodic accretion model was secondary.

5. CONCLUSION

We have analyzed, the Fermi-LAT data of Blazar S2 0109+22 from 2008 to 2022. Four different methods have been employed to search for the periodicity. We have found a γ -ray QPO behavior of ~ 600 days with a significance $\sim 3.5\sigma$ from MJD 56600 to 59974. Within 54682-56600 MJD, we suggested that turbulence from the accretion disk affected the jet radiation and disrupts the periodic variability. The distance between two black holes, according to our calculations, was $\sim 1.25 \times 10^{16} cm$. The total range of the two components of Doppler factor in the lighthouse model was

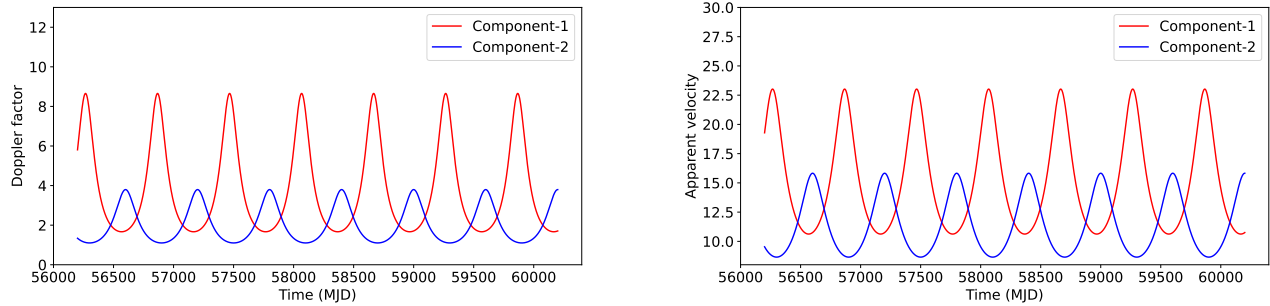


Figure 8. The top and bottom panel indicate the changes of Doppler factor and apparent velocity, respectively. The red and blue lines show the primary black hole (component-1) and the secondary black hole (component-2), respectively.

Table 3. Parameters for the Lighthouse Model.

Parameter	Value
Γ^*	35
T_{obs}	600 days
ψ_1	$7.43 \pm 0.08^\circ$
ϕ_1^*	80°
ψ_2	$9.91 \pm 0.03^\circ$
ϕ_2^*	240°
i	$3.07 \pm 0.08^\circ$
f_{b1}	$(0.42 \pm 0.08) \times 10^{-3}$
f_{b2}	$(0.49 \pm 0.02) \times 10^{-2}$
quiescent level	$(0.12 \pm 0.002) \times 10^{-7} \text{ ph cm}^{-2} \text{ s}^{-1}$

NOTE— Γ is refer to Wang et al. (2022). The superscript ”
* ” indicates the frozen parameter in fit.

Software: Astropy (Astropy Collaboration et al. 2022), Fermitools, REDFIT (Schulz & Mudsee 2002), iminuit (Dembinski & et al. 2020), JetSet (Tramacere 2020)

$1.10 < \delta < 8.66$. We have also obtained the total apparent velocity range with $8.65 < \beta_{app} < 23.02$, which indicated that this was a superluminal source. Therefore, it was possible that Blazar S2 0109+22 was a binary black hole system with a dual jet structure and a periodic accretion rate. Further credible data will be needed to support this quasi-periodic behavior, and we will continue tracking it in a future work.

Acknowledgments

We thank the anonymous referee for providing constructive comments and suggestions. This work was partly supported by the National Science Foundation of China (12263007 and 12233006), the High-level talent support program of Yunnan Province.

Facilities: Fermi (LAT)

REFERENCES

- Abdollahi, S., Acero, F., Ackermann, M., et al. 2020, *ApJS*, 247, 33, doi: [10.3847/1538-4365/ab6bcb](https://doi.org/10.3847/1538-4365/ab6bcb)
- Abramowicz, M. A., Karas, V., Kluzniak, W., Lee, W. H., & Rebusco, P. 2003, *PASJ*, 55, 467, doi: [10.1093/pasj/55.2.467](https://doi.org/10.1093/pasj/55.2.467)
- Ackermann, M., Ajello, M., Albert, A., et al. 2015, *ApJL*, 813, L41, doi: [10.1088/2041-8205/813/2/L41](https://doi.org/10.1088/2041-8205/813/2/L41)
- Arévalo, P., & Uttley, P. 2006, *MNRAS*, 367, 801, doi: [10.1111/j.1365-2966.2006.09989.x](https://doi.org/10.1111/j.1365-2966.2006.09989.x)
- Astropy Collaboration, Price-Whelan, A. M., Lim, P. L., et al. 2022, *ApJ*, 935, 167, doi: [10.3847/1538-4357/ac7c74](https://doi.org/10.3847/1538-4357/ac7c74)
- Atwood, W. B., Abdo, A. A., Ackermann, M., et al. 2009, *ApJ*, 697, 1071, doi: [10.1088/0004-637X/697/2/1071](https://doi.org/10.1088/0004-637X/697/2/1071)
- Baluev, R. V. 2008, *MNRAS*, 385, 1279, doi: [10.1111/j.1365-2966.2008.12689.x](https://doi.org/10.1111/j.1365-2966.2008.12689.x)
- Bednarek, W. 1998, *A&A*, 336, 123, doi: [10.48550/arXiv.astro-ph/9804097](https://doi.org/10.48550/arXiv.astro-ph/9804097)
- Bhatta, G. 2017, *ApJ*, 847, 7, doi: [10.3847/1538-4357/aa86ed](https://doi.org/10.3847/1538-4357/aa86ed)
- Bhatta, G., & Dhital, N. 2020, *ApJ*, 891, 120, doi: [10.3847/1538-4357/ab7455](https://doi.org/10.3847/1538-4357/ab7455)
- Bhatta, G., Zola, S., Stawarz, L., et al. 2016, *ApJ*, 832, 47, doi: [10.3847/0004-637X/832/1/47](https://doi.org/10.3847/0004-637X/832/1/47)
- Blandford, R. D., & Levinson, A. 1995, *ApJ*, 441, 79, doi: [10.1086/175338](https://doi.org/10.1086/175338)
- Blandford, R. D., & Payne, D. G. 1982, *MNRAS*, 199, 883, doi: [10.1093/mnras/199.4.883](https://doi.org/10.1093/mnras/199.4.883)
- Blandford, R. D., & Znajek, R. L. 1977, *MNRAS*, 179, 433, doi: [10.1093/mnras/179.3.433](https://doi.org/10.1093/mnras/179.3.433)
- Böttcher, M., Reimer, A., Sweeney, K., & Prakash, A. 2013, *ApJ*, 768, 54, doi: [10.1088/0004-637X/768/1/54](https://doi.org/10.1088/0004-637X/768/1/54)
- Cai, J. T., Kurtanidze, S. O., Liu, Y., et al. 2022, *ApJS*, 260, 47, doi: [10.3847/1538-4365/ac666b](https://doi.org/10.3847/1538-4365/ac666b)
- Ciprini, S., Tosti, G., Teräsraanta, H., & Aller, H. D. 2004, *MNRAS*, 348, 1379, doi: [10.1111/j.1365-2966.2004.07467.x](https://doi.org/10.1111/j.1365-2966.2004.07467.x)
- Covino, S., Sandrinelli, A., & Treves, A. 2019, *MNRAS*, 482, 1270, doi: [10.1093/mnras/sty2720](https://doi.org/10.1093/mnras/sty2720)
- Dai, B. Z., Xie, G. Z., Li, K. H., et al. 2001, *AJ*, 122, 2901, doi: [10.1086/324450](https://doi.org/10.1086/324450)
- Dai, B. Z., Li, X. H., Liu, Z. M., et al. 2009, *MNRAS*, 392, 1181, doi: [10.1111/j.1365-2966.2008.14137.x](https://doi.org/10.1111/j.1365-2966.2008.14137.x)
- Dai, B.-z., Zeng, W., Jiang, Z.-j., et al. 2015, *ApJS*, 218, 18, doi: [10.1088/0067-0049/218/2/18](https://doi.org/10.1088/0067-0049/218/2/18)
- Davis, M. M. 1971, *AJ*, 76, 980, doi: [10.1086/111211](https://doi.org/10.1086/111211)
- Dembinski, H., & et al., P. O. 2020, doi: [10.5281/zenodo.3949207](https://doi.org/10.5281/zenodo.3949207)
- Donea, A.-C., & Protheroe, R. J. 2003, *Astroparticle Physics*, 18, 377, doi: [10.1016/S0927-6505\(02\)00155-X](https://doi.org/10.1016/S0927-6505(02)00155-X)
- Emmanoulopoulos, D., McHardy, I. M., & Papadakis, I. E. 2013, *MNRAS*, 433, 907, doi: [10.1093/mnras/stt764](https://doi.org/10.1093/mnras/stt764)
- Fan, J. H., Xu, W., Pan, J., & Yuan, Y. H. 2011, in *Jets at All Scales*, ed. G. E. Romero, R. A. Sunyaev, & T. Belloni, Vol. 275, 164–167, doi: [10.1017/S1743921310015875](https://doi.org/10.1017/S1743921310015875)
- Fan, J.-H., Yang, J.-H., Liu, Y., & Zhang, J.-Y. 2013, *Research in Astronomy and Astrophysics*, 13, 259, doi: [10.1088/1674-4527/13/3/002](https://doi.org/10.1088/1674-4527/13/3/002)
- Fan, J. H., Liu, Y., Yuan, Y. H., et al. 2007, *A&A*, 462, 547, doi: [10.1051/0004-6361:20054775](https://doi.org/10.1051/0004-6361:20054775)
- Fan, J. H., Kurtanidze, S. O., Liu, Y., et al. 2021, *ApJS*, 253, 10, doi: [10.3847/1538-4365/abd32d](https://doi.org/10.3847/1538-4365/abd32d)
- Ferraz-Mello, S. 1981, *AJ*, 86, 619, doi: [10.1086/112924](https://doi.org/10.1086/112924)
- Foreman-Mackey, D., Agol, E., Ambikasaran, S., & Angus, R. 2017, *AJ*, 154, 220, doi: [10.3847/1538-3881/aa9332](https://doi.org/10.3847/1538-3881/aa9332)
- Foster, G. 1995, *AJ*, 109, 1889, doi: [10.1086/117416](https://doi.org/10.1086/117416)
- . 1996, *AJ*, 112, 1709, doi: [10.1086/118137](https://doi.org/10.1086/118137)
- Gandhi, P. 2009, *ApJL*, 697, L167, doi: [10.1088/0004-637X/697/2/L167](https://doi.org/10.1088/0004-637X/697/2/L167)
- Gierliński, M., Middleton, M., Ward, M., & Done, C. 2008, *Nature*, 455, 369, doi: [10.1038/nature07277](https://doi.org/10.1038/nature07277)
- Horák, J. 2008, *A&A*, 486, 1, doi: [10.1051/0004-6361:20078305](https://doi.org/10.1051/0004-6361:20078305)
- Ingram, A., & van der Klis, M. 2015, *MNRAS*, 446, 3516, doi: [10.1093/mnras/stu2373](https://doi.org/10.1093/mnras/stu2373)
- Kelly, B. C., Becker, A. C., Sobolewska, M., Siemiginowska, A., & Uttley, P. 2014, *ApJ*, 788, 33, doi: [10.1088/0004-637X/788/1/33](https://doi.org/10.1088/0004-637X/788/1/33)
- King, O. G., Hovatta, T., Max-Moerbeck, W., et al. 2013, *MNRAS*, 436, L114, doi: [10.1093/mnrasl/slt125](https://doi.org/10.1093/mnrasl/slt125)
- Kushwaha, P., Sarkar, A., Gupta, A. C., Tripathi, A., & Wiita, P. J. 2020, *MNRAS*, 499, 653, doi: [10.1093/mnras/staa2899](https://doi.org/10.1093/mnras/staa2899)
- Lehto, H. J., & Valtonen, M. J. 1996, *ApJ*, 460, 207, doi: [10.1086/176962](https://doi.org/10.1086/176962)
- Li, H.-Z., Gao, Q.-G., Qin, L.-H., Yi, T.-F., & Chen, Q.-R. 2022, *Research in Astronomy and Astrophysics*, 22, 055017, doi: [10.1088/1674-4527/ac630e](https://doi.org/10.1088/1674-4527/ac630e)
- Liska, M., Hesp, C., Tchekhovskoy, A., et al. 2018, *MNRAS*, 474, L81, doi: [10.1093/mnrasl/slx174](https://doi.org/10.1093/mnrasl/slx174)
- Liu, F. K., Zhao, G., & Wu, X.-B. 2006, *ApJ*, 650, 749, doi: [10.1086/507267](https://doi.org/10.1086/507267)
- Lomb, N. R. 1976, *Ap&SS*, 39, 447, doi: [10.1007/BF00648343](https://doi.org/10.1007/BF00648343)
- Lyubarskii, Y. E. 1997, *MNRAS*, 292, 679, doi: [10.1093/mnras/292.3.679](https://doi.org/10.1093/mnras/292.3.679)
- MAGIC Collaboration, Ansoldi, S., Antonelli, L. A., et al. 2018, *MNRAS*, 480, 879, doi: [10.1093/mnras/sty1753](https://doi.org/10.1093/mnras/sty1753)

- Maraschi, L., Ghisellini, G., & Celotti, A. 1992, *ApJL*, 397, L5, doi: [10.1086/186531](https://doi.org/10.1086/186531)
- Massaro, E., Tramacere, A., Perri, M., Giommi, P., & Tosti, G. 2006, *A&A*, 448, 861, doi: [10.1051/0004-6361:20053644](https://doi.org/10.1051/0004-6361:20053644)
- O'Neill, S., Kiehlmann, S., Readhead, A. C. S., et al. 2022, *ApJL*, 926, L35, doi: [10.3847/2041-8213/ac504b](https://doi.org/10.3847/2041-8213/ac504b)
- Owen, F. N., & Mufson, S. L. 1977, *AJ*, 82, 776, doi: [10.1086/112124](https://doi.org/10.1086/112124)
- Padovani, P. 2017, *Nature Astronomy*, 1, 0194, doi: [10.1038/s41550-017-0194](https://doi.org/10.1038/s41550-017-0194)
- Padovani, P., Alexander, D. M., Assef, R. J., et al. 2017, *A&A Rv*, 25, 2, doi: [10.1007/s00159-017-0102-9](https://doi.org/10.1007/s00159-017-0102-9)
- Pauliny-Toth, I. I. K., Kellermann, K. I., Davis, M. M., Fomalont, E. B., & Shaffer, D. B. 1972, *AJ*, 77, 265, doi: [10.1086/111278](https://doi.org/10.1086/111278)
- Peñil, P., Domínguez, A., Buson, S., et al. 2020, *ApJ*, 896, 134, doi: [10.3847/1538-4357/ab910d](https://doi.org/10.3847/1538-4357/ab910d)
- Perez, C. A., Silbergleit, A. S., Wagoner, R. V., & Lehr, D. E. 1997, *ApJ*, 476, 589, doi: [10.1086/303658](https://doi.org/10.1086/303658)
- Pica, A. J. 1977, *AJ*, 82, 935, doi: [10.1086/112150](https://doi.org/10.1086/112150)
- Qian, S.-J., Kudryavtseva, N. A., Britzen, S., et al. 2007, *ChJA&A*, 7, 364, doi: [10.1088/1009-9271/7/3/05](https://doi.org/10.1088/1009-9271/7/3/05)
- Ren, G.-W., Ding, N., Zhang, X., et al. 2021, *MNRAS*, 506, 3791, doi: [10.1093/mnras/stab1739](https://doi.org/10.1093/mnras/stab1739)
- Ren, H. X., Cerruti, M., & Sahakyan, N. 2023, *A&A*, 672, A86, doi: [10.1051/0004-6361/202244754](https://doi.org/10.1051/0004-6361/202244754)
- Rezzolla, L., Yoshida, S., Maccarone, T. J., & Zanotti, O. 2003, *MNRAS*, 344, L37, doi: [10.1046/j.1365-8711.2003.07018.x](https://doi.org/10.1046/j.1365-8711.2003.07018.x)
- Ricci, L., Boccardi, B., Nokhrina, E., et al. 2022, *A&A*, 664, A166, doi: [10.1051/0004-6361/202243958](https://doi.org/10.1051/0004-6361/202243958)
- Romero, G., & Gutiérrez, E. 2020, *Universe*, 6, 99, doi: [10.3390/universe6070099](https://doi.org/10.3390/universe6070099)
- Sandrinelli, A., Covino, S., & Treves, A. 2014, *ApJL*, 793, L1, doi: [10.1088/2041-8205/793/1/L1](https://doi.org/10.1088/2041-8205/793/1/L1)
- Sandrinelli, A., Covino, S., Treves, A., et al. 2017, *A&A*, 600, A132, doi: [10.1051/0004-6361/201630288](https://doi.org/10.1051/0004-6361/201630288)
- Scargle, J. D. 1982, *ApJ*, 263, 835, doi: [10.1086/160554](https://doi.org/10.1086/160554)
- Scargle, J. D., Steiman-Cameron, T., Young, K., et al. 1993, *ApJL*, 411, L91, doi: [10.1086/186920](https://doi.org/10.1086/186920)
- Schnittman, J., & Bertschinger, E. 2004, in *American Institute of Physics Conference Series*, Vol. 714, X-ray Timing 2003: Rossi and Beyond, ed. P. Kaaret, F. K. Lamb, & J. H. Swank, 40–43, doi: [10.1063/1.1780996](https://doi.org/10.1063/1.1780996)
- Schulz, M., & Mudelsee, M. 2002, *Computers and Geosciences*, 28, 421, doi: [10.1016/S0098-3004\(01\)00044-9](https://doi.org/10.1016/S0098-3004(01)00044-9)
- Sikora, M., Begelman, M. C., & Rees, M. J. 1994, *ApJ*, 421, 153, doi: [10.1086/173633](https://doi.org/10.1086/173633)
- Sillanpaa, A., Haarala, S., Valtonen, M. J., Sundelius, B., & Byrd, G. G. 1988, *ApJ*, 325, 628, doi: [10.1086/166033](https://doi.org/10.1086/166033)
- Sillanpaa, A., Teerikorpi, P., Haarala, S., et al. 1985, *A&A*, 147, 67
- Smith, K. L., Mushotzky, R. F., Boyd, P. T., & Wagoner, R. V. 2018, *ApJL*, 860, L10, doi: [10.3847/2041-8213/aac88c](https://doi.org/10.3847/2041-8213/aac88c)
- Smith, K. L., Tandon, C. R., & Wagoner, R. V. 2021, *ApJ*, 906, 92, doi: [10.3847/1538-4357/abc9b7](https://doi.org/10.3847/1538-4357/abc9b7)
- Sobacchi, E., Sormani, M. C., & Stamerra, A. 2017, *MNRAS*, 465, 161, doi: [10.1093/mnras/stw2684](https://doi.org/10.1093/mnras/stw2684)
- Tavecchio, F., Maraschi, L., & Ghisellini, G. 1998, *ApJ*, 509, 608, doi: [10.1086/306526](https://doi.org/10.1086/306526)
- Timmer, J., & Koenig, M. 1995, *A&A*, 300, 707
- Tramacere, A. 2020, *JetSeT: Numerical modeling and SED fitting tool for relativistic jets*, *Astrophysics Source Code Library*, record ascl:2009.001. <http://ascl.net/2009.001>
- Tramacere, A., Giommi, P., Perri, M., Verrecchia, F., & Tosti, G. 2009, *A&A*, 501, 879, doi: [10.1051/0004-6361/200810865](https://doi.org/10.1051/0004-6361/200810865)
- Tramacere, A., Massaro, E., & Taylor, A. M. 2011, *ApJ*, 739, 66, doi: [10.1088/0004-637X/739/2/66](https://doi.org/10.1088/0004-637X/739/2/66)
- Tripathi, A., Gupta, A. C., Aller, M. F., et al. 2021, *MNRAS*, 501, 5997, doi: [10.1093/mnras/stab058](https://doi.org/10.1093/mnras/stab058)
- Urry, C. M., & Padovani, P. 1995, *PASP*, 107, 803, doi: [10.1086/133630](https://doi.org/10.1086/133630)
- Valtonen, M. J., Lehto, H. J., Sillanpää, A., et al. 2006, *ApJ*, 646, 36, doi: [10.1086/504884](https://doi.org/10.1086/504884)
- Valtonen, M. J., Lehto, H. J., Nilsson, K., et al. 2008, *Nature*, 452, 851, doi: [10.1038/nature06896](https://doi.org/10.1038/nature06896)
- Villata, M., Raiteri, C. M., Sillanpaa, A., & Takalo, L. O. 1998, *MNRAS*, 293, L13, doi: [10.1046/j.1365-8711.1998.01244.x](https://doi.org/10.1046/j.1365-8711.1998.01244.x)
- Wagner, S. J., & Witzel, A. 1995, *ARA&A*, 33, 163, doi: [10.1146/annurev.aa.33.090195.001115](https://doi.org/10.1146/annurev.aa.33.090195.001115)
- Wang, G. G., Cai, J. T., & Fan, J. H. 2022, *ApJ*, 929, 130, doi: [10.3847/1538-4357/ac5b08](https://doi.org/10.3847/1538-4357/ac5b08)
- Wills, D., & Wills, B. J. 1976, *ApJS*, 31, 143, doi: [10.1086/190378](https://doi.org/10.1086/190378)
- Xiao, H., Fan, J., Ouyang, Z., et al. 2022, *ApJ*, 936, 146, doi: [10.3847/1538-4357/ac887f](https://doi.org/10.3847/1538-4357/ac887f)
- Xiao, H., Fan, J., Yang, J., et al. 2019, *Science China Physics, Mechanics, and Astronomy*, 62, 129811, doi: [10.1007/s11433-018-9371-x](https://doi.org/10.1007/s11433-018-9371-x)
- Yang, S., Yan, D., Zhang, P., Dai, B., & Zhang, L. 2021, *ApJ*, 907, 105, doi: [10.3847/1538-4357/abcbff](https://doi.org/10.3847/1538-4357/abcbff)
- Young, K., & Scargle, J. D. 1996, *ApJ*, 468, 617, doi: [10.1086/177720](https://doi.org/10.1086/177720)

- Zhang, B.-K., Zhao, X.-Y., Wang, C.-X., & Dai, B.-Z. 2014, *Research in Astronomy and Astrophysics*, 14, 933, doi: [10.1088/1674-4527/14/8/004](https://doi.org/10.1088/1674-4527/14/8/004)
- Zhang, H., Yan, D., & Zhang, L. 2022, *ApJ*, 930, 157, doi: [10.3847/1538-4357/ac679e](https://doi.org/10.3847/1538-4357/ac679e)
- Zhang, H., Yang, S., & Dai, B. 2023, *ApJ*, 946, 52, doi: [10.3847/1538-4357/acbe37](https://doi.org/10.3847/1538-4357/acbe37)
- Zhang, P., Zhang, P.-f., Yan, J.-z., Fan, Y.-z., & Liu, Q.-z. 2017a, *ApJ*, 849, 9, doi: [10.3847/1538-4357/aa8d6e](https://doi.org/10.3847/1538-4357/aa8d6e)
- Zhang, P.-f., Yan, D.-h., Liao, N.-h., & Wang, J.-c. 2017b, *ApJ*, 835, 260, doi: [10.3847/1538-4357/835/2/260](https://doi.org/10.3847/1538-4357/835/2/260)
- Zhang, P.-f., Yan, D.-h., Liao, N.-h., et al. 2017c, *ApJ*, 842, 10, doi: [10.3847/1538-4357/aa7465](https://doi.org/10.3847/1538-4357/aa7465)
- Zhang, P.-F., Yan, D.-H., Zhou, J.-N., et al. 2017d, *ApJ*, 845, 82, doi: [10.3847/1538-4357/aa7ecd](https://doi.org/10.3847/1538-4357/aa7ecd)
- Zhang, P.-f., Zhang, P., Liao, N.-h., et al. 2018, *ApJ*, 853, 193, doi: [10.3847/1538-4357/aaa29a](https://doi.org/10.3847/1538-4357/aaa29a)
- Zhang, X. 2021, *MNRAS*, 502, 1158, doi: [10.1093/mnras/stab019](https://doi.org/10.1093/mnras/stab019)
- . 2022, *MNRAS*, 512, 1003, doi: [10.1093/mnras/stac540](https://doi.org/10.1093/mnras/stac540)
- Zhou, J., Wang, Z., Chen, L., et al. 2018, *Nature Communications*, 9, 4599, doi: [10.1038/s41467-018-07103-2](https://doi.org/10.1038/s41467-018-07103-2)
- Zhou, X.-L., Yuan, W., Pan, H.-W., & Liu, Z. 2015, *ApJL*, 798, L5, doi: [10.1088/2041-8205/798/1/L5](https://doi.org/10.1088/2041-8205/798/1/L5)